UNIVERSITY OF LEEDS

This is a repository copy of *Stereo imaging of crystal growth*.

White Rose Research Online URL for this paper:
http://eprints.whiterose.ac.uk/94599/

Version: Accepted Version

Article:
Ma, CY, Liu, JJ and Wang, XZ (2016) Stereo imaging of crystal growth. AIChE Journal, 62 (1). pp. 18-25. ISSN 0001-1541

https://doi.org/10.1002/aic.15041

Reuse
Unless indicated otherwise, fulltext items are protected by copyright with all rights reserved. The copyright exception in section 29 of the Copyright, Designs and Patents Act 1988 allows the making of a single copy solely for the purpose of non-commercial research or private study within the limits of fair dealing. The publisher or other rights-holder may allow further reproduction and re-use of this version - refer to the White Rose Research Online record for this item. Where records identify the publisher as the copyright holder, users can verify any specific terms of use on the publisher's website.

Takedown
If you consider content in White Rose Research Online to be in breach of UK law, please notify us by emailing eprints@whiterose.ac.uk including the URL of the record and the reason for the withdrawal request.

eprints@whiterose.ac.uk
https://eprints.whiterose.ac.uk/

Submitted to AIChE J as an AIChE Letter

Stereo Imaging of Crystal Growth

Cai Y. Ma[1], Jing J. Liu[2] and Xue Z. Wang[2,1,*]

[1]Institute of Particle Science and Engineering, School of Chemical and Process Engineering, University of Leeds, Leeds LS2 9JT, United Kingdom

[2]School of Chemistry and Chemical Engineering, South China University of Technology, Guangzhou 510640, PR China

*** Correspondence author:**

Prof Xue Z Wang

China One Thousand Talent Scheme Professor
School of Chemistry and Chemical Engineering
South China University of Technology
381 Wushan Rd, Tianhe District
Guangzhou, PR China 510641
Tel: +86 20 8711 4000, Fax: +86 20 8711 4000, Email; xuezhongwang@scut.edu.cn

&

Personal Chair in Intelligent Measurement and Control
Institute of Particle Science and Engineering
School of Chemical and Process Engineering
University of Leeds
Leeds LS2 9JT, UK
Tel +44 113 343 2427, Fax +44 113 343 2384, Email x.z.wang@leeds.ac.uk

Significance

A methodology that directly images the full three-dimensional shape of crystals within a crystalliser is reported. It is based on the mathematical principle that if the two-dimensional images of an object are obtained from two or more different angles, the full three-dimensional crystal shape could be reconstructed. A prototype instrument is built and proof of concept study carried out to demonstrate the potentials in using the system for three-dimensional measurement of crystal shape and shape distribution. It is our belief that 3D measurement of crystal shape represents a significant step forward from existing work of 2D measurement of crystal morphology and is potentially of great significance to research towards closed-loop control of crystal morphology.

Keywords: Stereo imaging, Crystal shape, Three-dimensional shape reconstruction, Image analysis, Crystallisation Process Control

1. Introduction

Particle shape is known to be extremely important to many pharmaceuticals, biopharmaceuticals, human health products and speciality chemicals in solid form. In the pharmaceutical industry, particle properties such as dry powder density, cohesion, and flowability, etc. can be affected by crystal morphology, which plays an important role in a company's ability to formulate drug particles into finished products. Moreover, crystal morphology can affect drug dissolution, potentially affecting finished product bioavailability and, in some extreme conditions, leading to a company to lose the production license of a drug.

Despite its significant potential importance, the direct characterisation of particle shape has been quite limited largely relying on off-line instruments. For quite some time there have been no effective instruments capable of providing real-time information on particle shape particularly with the capability for use during the processing of particles in unit operations such as crystallisation, precipitation, granulation and milling (dry or wet). During the last decades, well-developed and studied PAT (process analytical technology) techniques such as acoustic, and mid and near infrared spectroscopy and laser diffraction have been used in process monitoring, these techniques cannot give detailed information on particle shape though some of them have shown to be able to distinguish between different polymorphs with careful spectral data analysis using chemometrics. Overall, the inability in the measurement of particle shape and growth rates in individual faces has greatly restricted the development and implementation of monitoring and control of particle shape for these particle formulation and processing systems.

In recent years, several research groups and industrial companies have found that it is feasible to use on-line two-dimensional (2D) imaging for particle shape measurement, and initiated research activities[1-15]. Rawlings and co-workers carried out research on the measurement of crystal size and shape distributions using on-line video images[15]. Wilkinson et al. from GlaxoSmithKline developed a prototype on-line, non-invasive microscopy imaging system[11] for monitoring pharmaceutical crystallisation. AstraZenaca[14] tested the use of a commercially available imaging probe named as PVM. In medical and biological areas, miniature CCD cameras were used to develop imaging systems. Gorpas et al.[16] developed a volumetric method, using a binocular machine vision system with a structured light projector, to reconstruct three-dimensional (3D) tumour surfaces (ca. 10 mm in size). An imaging system using a flow through cell with one camera and two mirrors was developed to obtain 3D information of crystals grown from solution[17]. A few of three cameras imaging systems were also developed to characterise 3D shape of free-falling particles (100μm ~ 4mm)[18] or 3D information of a wound area[19]. However, all these binocular and three-camera imaging systems are not designed to be used in a reactor for direct measurement of crystal size and shape evolution and the objects to be characterised are normally at millimeter scale, hence not being suitable for micron-sized crystals. Interactive systems that allow users to control and manipulate real-world objects within a remote real environment are known as teleoperator or telerobotic systems[20]. Such systems are often used in medical applications to confirm diagnosis and make telepresence surgery. Some 2D/3D endoscopes have been developed for these purposes (see for example[20-22]) with the most known ones being da Vinci telerobotic surgical system[21] and ZEUS[22]. Such systems are controlled by surgeons remotely by viewing virtual surgical site with stereoscopic system and controlling stereoscopic camera and robot surgical armaments. However, these imaging systems still have significant limitations in terms of their image processing capabilities and how to link the information for shape monitoring and control. In fact at the moment they are mainly used to display information to operators and store data onto hard drive. Nevertheless, we believe that with the active research activities internationally and the great interest from instrument companies and end-users, before long the image processing capabilities will improve significantly, thus opening up new commercial opportunities for on-line monitoring and control of crystal size distributions based on shape evolution.

Despite the several research and development programmes internationally, all the work on crystal size and shape measurements was restricted to 2D imaging. Although 2D shape is already a major step from the traditional characterisation of particles based only on a volume equivalent

diameter of a sphere, being able to measure 3D shape will be of much greater scientific and industrial significance. Some microscopic systems such as confocal microscopy are able to provide 3D information of a particle by scanning many thin sections of the sample[23]. Other techniques can also be used to provide some useful 3D information of particles off-line such as scanning electron microscopy (SEM) and electron and X-ray tomography. However, these systems are not practical for 3D on-line measurements due to the very low speed in operation. Mazzotti and co-workers[24,25] designed a flow through microscope with a mirror configuration, hence the passing particles can be viewed from two directions. They applied the system to ascorbic acid crystals for extracting crystal length, width and depth information. A flow through microscope system was also used to obtain high quality images with regard to particle sharpness[26]. The boundary curve of 2D crystal projection was used to estimate 3D shape. Intensive research and development has been carried out to obtain 3D topographical data of objects in robotics and machine vision areas with the objects at meter or millimeter scale. Several optical, non-contact methods have been developed for a wide range of applications, such as moire methods (shadow and projection), fast-Fourier transform approaches, stereo imaging etc. Stereo imaging has the advantage of providing more direct, unambiguous and quantitative depth information, and it can be used for a very wide range of applications in academic research, industry and daily life in addition to the applications of 3D measurement. Most approaches to the application of stereo vision utilise the human vision system to establish a model for the camera system. For stereo imaging system, many different camera-object geometries have been studied and used for specific applications such as the common parallel camera optical axes, the converging (nonparallel) camera optical axes, etc. To extract 3D information from the recorded stereo image pairs for 3D reconstruction of objects, it is necessary to find disparities among a series of corresponding points between a pair of stereo images taken from the same scene. There are many matching techniques and corresponding algorithms which can be generally divided into three categories: area-based, feature-based, and their combination. In general, feature-based techniques yield a better match more stably and accurately than other techniques. Two types of features commonly used are point-like features such as corners and line segments[27]. Overall, the use of single 2D images or stereo images for constructing 3D shape of crystals at micron size scale is still very limited.

In this paper, a proof of concept study has been carried out to demonstrate the great potentials in using the system for the 3D measurements of particles at micron scale. The basic mode of the operation is based on the mathematical principle that if the 2D images of an object are obtained from two different angles, the full 3D particle shape can be recovered. In the following sections, the methodology of 3D stereovision imaging system for the characterisation of crystal shape is briefly described. Then the stereovision imaging system is developed with some case studies. Finally, some concluding remarks and further development are given.

2. The Methodology

A two-camera system is proposed, which places two cameras at a pre-defined angle (stereo angle). The two cameras focus on the same sample volume with the identical camera parameters. The stereo image pairs can be obtained via these two cameras when shuttering at a synchronised instant. The obtained stereo image frames are processed using a multi-scale segmentation algorithm[2] or other pre-processing methods. Using corner/edge/line detection[28,29], the corners, edges and lines of the crystals from the processed images can be identified. A feature-based matching algorithm (see for example[27]) can be used to identify the corresponding left and right features (corners, edges, lines). The 3D coordinates of crystal shape can then be reconstructed with the identified corresponding corners, edges or lines using a stereo triangulation algorithm. The obtained 3D crystal shape can be further processed for the characterisation of crystals such as face growth rates, shape factor, surface area, volume and size distribution.

3. Stereovision 3D imaging system

The schematic diagram of a stereo imaging system is shown in Figure 1. The system can be composed of a reactor or a growth cell for crystal growth under accurate control of heating and

cooling conditions and a stereovision imaging system for capturing stereo image frames. The recorded stereo image pairs are stored onto a PC for further image analysis and 3D reconstruction.

Technique to use stereo cameras (two cameras) for the reconstruction of 3D vision is directly related to human vision system, i.e. two cameras mimics our left and right eyes and 3D reconstruction software mimics the fast image processing of our brain. Therefore, stereovision technique is not new in any aspect and has been widely used in machine vision such as vehicle and person identification, product manufacturing etc. though most of them positioned two cameras in parallel. In chemical processing area, stereovision systems for 3D reconstruction of particles in micron size scale in reactors are still rare because of the technique challenges when the object size is reduced from millimeters or meters to microns. The proposed stereovision 3D imaging system in this paper is to face the challenges and provide a practical tool for 3D reconstruction of micron-sized particles in reactors. The built-up stereo imaging system includes a 3D imaging block (two cameras with two telecentric lenses), a strobe control/pulse generator for synchronising cameras and lights, a light source, a light controller with strobe triggering pulse for synchronising cameras and lights, a crystalliser, and a PC with image acquisition software and image processing software for 3D shape reconstruction and post-processing. The imaging system has a spatial resolution of 3.45 μm with the current selection of cameras and lenses. The system can capture up to 6 frames per second with each image having a resolution of 2448×2050 pixels.

4. 3D shape reconstruction from 2D stereo images

With the recorded image pairs, each image is undertaken several image processing steps including pre-processing such as the adjustment of image contrast, edge/corner extraction, and the identification of edge/corner correspondence for 3D reconstruction. Using the multi-scale segmentation method[2], the crystals from each image of an image pairs can be identified and numbered for further processing. The central coordinates of the numbered crystals are calculated. The paired crystals between the two images in an image pairs can then be found by comparing the central coordinates of the numbered crystals in one image against those in another image with a displacement distance due to the angled stereo cameras. The identified crystal pairs will be further processed to reconstruct 3D shape. In some cases, crystal pairs may be fully or partially overlapped, which will be discarded as there exist very few algorithms being able to separate overlapped (or aggregated) crystals effectively and accurately at the moment. According to the different features from different crystal shapes such as needle-like, plate-like, rod-like etc., the corner correspondence between the identified crystal pairs can be established. This method can avoid the search of the whole image to obtain the matched corners, hence improving processing speed and quality.

For 3D reconstruction from 2D stereo images, in addition to stereo matching to obtain the correspondence of the identified crystal corners in the paired images taken from the same scene, the reconstruction of an object from the correspondence can be achieved by using the triangulation method. For the 3D coordinates of a corner, the 3D coordinates (X, Y, Z) of this corner is a function of the coordinates of the two 2D images (x_1, y_1, x_2, y_2), stereo angle (α), the total distance (L) between a subject and camera, other properties such as resolution (σ), magnification (Δ) etc.

$$(X, Y, Z) = f(x_1, y_1, x_2, y_2, \alpha, \sigma, \Delta, L, \ldots) \quad (1)$$

In the current imaging configurations of the cameras and lenses, the stereo angle between the two camera optic axes is fixed at 22 degrees and the total distance L including the lens working distance, lens length and camera flange focal distance, has a value of 147.726 mm. The magnification of the lenses, Δ, is 2 times with a resolution σ of 4.65 μm. The obtained equation for the calculation of 3D coordinates of a corner or point from the two 2D images is as follows.

$$\begin{bmatrix} X \\ Y \\ Z \end{bmatrix} = \begin{bmatrix} a_{11} & 0 & 0 \\ 0 & a_{22} & 0 \\ 0 & 0 & a_{33} \end{bmatrix} \begin{bmatrix} b_1 \\ b_2 \\ b_3 \end{bmatrix} \quad (2)$$

where

$$\begin{bmatrix} b_1 \\ b_2 \\ b_3 \end{bmatrix} = \begin{bmatrix} \frac{\sin\frac{\alpha}{2}}{\sin\alpha} \\ 1 \\ \frac{\cos\frac{\alpha}{2}}{\cos\alpha} \end{bmatrix} \tag{3}$$

$$\begin{bmatrix} a_{11} \\ a_{22} \\ a_{33} \end{bmatrix} = \begin{bmatrix} a_{10} + (x_1 + x_2)\frac{\sigma}{\Delta} \\ y_1 \frac{\sigma}{\Delta} \\ a_{30} + (x_2 - x_1)\frac{\sigma}{\Delta} \end{bmatrix} \tag{4}$$

with a_{10} = 74 mm and a_{30} = 54.5 mm. The reconstructed 3D particles are then used to calculate particle shape descriptors and also perform classification and clustering of particles.

Take a real needle-like crystal (a line segment in theory) as an example, suppose its real length is 1000 μm. However, it can be measured as 1000 μm on a 2D image only if the line is at an orientation perpendicular to the camera optic axis. If the line has an angle of ~60 degree against the optic axis, it can only be measured as having a length of 850 μm on a 2D image. Based on the camera model [4], 2D images pairs of the line can be computationally generated. With crystal pair identification and edge/corner detection, the coordinates of the end points for the paired lines on the 2D image can be used to reconstruct the 3D coordinates of the end points of the line, hence the line in real space. Using our algorithm the reconstructed 3D line has a length of 991 μm, which is about 1% from the real length of 1000 μm. It can be seen that it will present significant error if the 2D length of 850 μm for this line is used for further crystal characterisation. Furthermore, at the extreme configuration of a line that parallels to the camera optic axis, the line length on a 2D image will be close to zero. Other methods such as SEM, confocal microscopy can also be used to verify and assess the accuracy of the developed method.

For the image pairs captured from a plate-like crystal in a reactor (Figure 2(a)), the application of the multi-scale segmentation method and the crystal pairs identification procedure will identify the crystal pairs (Figure 2(b)) for further processing. Based on the features of a plate-like crystal, a parallel fitting procedure is applied to the identified crystal pairs to obtain the 2D coordinates of the corresponding corners (Figure 2(c)). Again, due to the plate-like crystal is not orientated perpendicular to the camera optic axis, the reconstructed crystal (Figure 2(d)) has larger length and width, hence larger area comparing to those from pure 2D calculations.

For an idealised crystal of L-glutamic acid (LGA) α-form, the same crystal pair identification procedure can be applied to the original 2D images (Figure 3(a)) and the identified crystal pairs were then processed with edge/corner detection and correspondence search. The reconstructed 3D shape of the LGA α-form crystal is shown in Figure 3(b). Note that with the help of crystal symmetrical features, the whole crystal shape of LGA α-form can be established from the reconstructed 3D shape which only represents a half of the real crystal in 3D space.

The typical stereo images of a sugar crystal are shown in Figure 3(c). After performing crystal pair identification, edge/corner detection and correspondence of the left and right images, the coordinates of the corresponding corners on left and right images were used to obtain the 3D shape of a sugar crystal (Figure 3(d)). Again, crystal symmetry can help to establish the whole 3D structure.

The typical images of potash alum crystals are illustrated in Figure 3(e) (left and right images). Crystal pair identification, edge/corner detection with some false corners being manually removed, and then correspondence processing were performed. With the corner coordinates, stereo triangulation can be used to calculate the corresponding 3D coordinates. After that, the 3D shape of the crystal was reconstructed as shown in Figure 3(g). For comparison purpose, the nine surfaces of the potash alum crystal on the 2D image were shown in Figure 3(f), each associated with a letter from A to I. By following the habit faces of potash alum crystals, i.e. 26 faces in 3 symmetrical face groups {100}, 110} and {111}, faces A – I in Fig. 3(f, g) are corresponding to the three face groups: one {100} face – A; four {110} faces – B, D, F, H; and four {111} faces – C, E, G, I. The crystal size in x, y and z directions were estimated from the 3D coordinates as 580, 588 and 277μm, respectively.

A proof of concept study under seeded cooling crystallisation conditions was carried out using an industrial compound with cuboid-like crystal shape to obtain the crystal growth rates of the individual faces. The captured stereo images from both cameras were processed to reconstruct the 3D shape of individual crystals, i.e. obtaining the 3D coordinates of all corners of a cuboid-like crystal and also the corresponding normal distances (x, y and z) between the centre of the crystal and the corresponding individual faces 1, 2 and 3. The 3D imaging system recorded the stereo images at a rate of one per second for a period of ~75 minutes (from the time of seeds being added at 70 min to the end of recording at 145 min). As the motion and rotation of crystals and also the crystal overlapping happened during the crystallisation process, in this study, some typical stereo images at a few time instances (75, 90, 100, 110, 120, 130 and 140 min), corresponding to each time point images of a time window of 5 minutes were selected for processing and 3D shape reconstruction. The normal distances of individual faces within the 5 minutes time window formed their distributions which then were used to obtain their corresponding mean normal distances. The mean normal distances of faces 1, 2 and 3 are plotted in Figure 4 with the corresponding fitted results as $x = 1.76\ t - 102.28\ \mu m$, $y = 1.94\ t - 99.02\ \mu m$ and $z = 1.25\ t - 78.35\ \mu m$, where t is the time (min), with fitting R^2 being 0.97, 0.99 and 0.98, respectively. From the linear relationship between the normal distances and crystallisation time, the crystal growth rates of three individual faces (face 1, 2 and 3) for the cuboid-like compound have constant values of 1.76, 1.94 and 1.25 µm/min, respectively.

The 3D reconstruction speed using the developed method depends on various factors such as quality of images, the complexity of the imaged crystals etc. Typically, reconstructing a 3D line, or a plate-like crystal, or a more complex shaped crystal requires from 1 to a few seconds using a desktop PC (duo core 2.0GHz processor and 3Gb RAM operating under Windows XP). To reconstruct all crystals from image pairs, the time required also depends on the number of paired crystals identified from an image pairs. In cooling crystallisation processes, the sampling times for images and temperature can be very fast (ca. < 1 s), but for concentration measurement typically from 30 s or longer. Therefore the 3D reconstruction processing time can be in the same order as the concentration measurement using attenuated total reflection - Fourier transform infrared (FTIR) spectroscopy. However, for fast crystallisation such as reactive crystallisation, high performance PC may be needed to speed up the processes of images and FTIR spectra, hence developing real-time on-line feedback control systems.

5. Final remarks

Crystal growth is primarily controlled by its surface chemistry which leads to various growth rates for different crystal faces. During crystallisation processes, surface chemistry for each face can also vary with operating conditions. Therefore, in order to develop real-time shape model predictive control [30-32], the on-line measurement of faceted crystal growth rates, from crystal shape evolution, during the crystallisation process becomes an essential and direct input into the population balance models including the unique morphological population balance model (MPB) [33,34]. With real-time on-line measurement of crystal shape/size evolution, together with a proper process optimisation and control technique, a real-time, on-line MPB-based closed-loop feedback control can be developed and applied to practical crystallisers, hence achieving the desired crystal properties of final products including shape and size distributions. In literature such as Kwon et al. [30-32], by combining PB model with measured faceted growth rates, a predictive control strategy was developed to control crystal shape and size of hen-egg-white (HEW) lysozyme. The on-line size (or aspect ratio) of HEW lysozyme crystals was obtained from imaging techniques such as particle vision and measurement (PVM) and Focused beam reflectance measurement (FBRM) which cannot provide 3D crystal shape evolution. As shown in Section 4, due to the continuous rotation of crystals in a crystalliser, the crystal orientation against the camera optic axis may generate great error. Therefore combining aspect ratio from PVM and FBRM 2D measurements with crystal morphology may not produce accurate crystal shape and size.

The existing process imaging systems can only record 2D images and some 3D systems in machine vision and medical applications have been applied only to large objects and/or the visualisation of 3D

images as an assistant to remote micro-surgery. The 3D stereovision imaging system presented in this paper is designed to record and reconstruct 3D shape of particles at micron size scale in reactors. The technique uses two cameras and two telecentric lenses to image different facets of a particle, and then to reconstruct the 3D shape. The reconstruction of 3D crystal shape from 2D stereo images can involve the following steps: raw stereo image pre-processing; corner/edge detection; correspondence establishment and triangulation for 3D calculations. The obtained 3D crystal shape can be used to characterise crystal properties such as face growth rates, shape factor, surface area, volume and size distribution. The case studies demonstrated that the instrument, together with the developed methodology, is potentially very useful for process and product quality monitoring and control of crystallisation processes in academic research and industrial applications including pharmaceuticals, agro-chemicals, dyes and pigments, food, detergents and formulation additives.

Acknowledgments

Financial support from the China One Thousand Talent Scheme and National Natural Science Foundation of China (NNSFC) under its Major Research Scheme of Meso-scale Mechanism and Control in Multi-phase Reaction Processes (project reference: 91434126) is acknowledged. The research reported in this paper has also benefited from previous work supported by the UK Engineering and Physical Sciences Research Council (EPSRC) for the projects of Shape (EP/C009541) and StereoVision (EP/E045707) and by the Technology Strategy Board (TSB) for the project High Value Manufacturing CGM (TP/BD059E).

Literature Cited

1. Calderon de Anda J, Wang XZ, Lai X, K.J. Roberts, K.H. Jennings, M.J. Wilkinson, D. Watson, D. Roberts . Real-time product morphology monitoring in crystallization using imaging technique. *AIChE J.* 2005;51(5):1406-1414.

2. Calderon de Anda J, Wang XZ, Roberts KJ. Multi-scale segmentation image analysis for the in-process monitoring of particle shape with batch crystallisers. *Chem Eng Sci.* 2005;60(4):1053-1065.

3. Kempkes M, Eggers J, Mazzotti M. Measurement of particle size and shape by FBRM and in situ microscopy. *Chem Eng Sci.* 2008;63(19):4656-4675.

4. Li RF, Thomson GB, White G, Wang XZ, De Anda JC, Roberts KJ. Integration of crystal morphology modeling and on-line shape measurement. *AIChE J.* 2006;52(6):2297-2305.

5. Patience DB, Rawlings JB. Particle-shape monitoring and control in crystallization processes. *AIChE J.* 2001;47(9):2125-2130.

6. Qu HY, Louhi-Kultanen M, Kallas J. In-line image analysis on the effects of additives in batch cooling crystallization. *J Cryst Growth.* 2006;289(1):286-294.

7. Scholl J, Bonalumi D, Vicum L, Mazzotti M, Muller M. In situ monitoring and modeling of the solvent-mediated polymorphic transformation of L-glutamic acid. *Cryst Growth Des.* 2006;6(4):881-891.

8. Wang XZ, Calderon De Anda J, Roberts KJ. Real-time measurement of the growth rates of individual crystal facets using imaging and image analysis: a feasibility study on needle-shaped crystals of L-glutamic acid. *Chem Eng Res Des.* 2007;85A:921-927.

9. Wang XZ, Calderon De Anda J, Roberts KJ, Li RF, Thomson GB, White G. Advances in on-line monitoring and control of the morphological and polymorphic forms of organic crystals grown from solution. *KONA.* 2005;23:69-85.

10. Wang XZ, Roberts KJ, Ma CY. Crystal growth measurement using 2D and 3D imaging and the perspectives for shape control. *Chem Eng Sci.* 2008;63(5):1171-1184.

11. Wilkinson MJ, Jennings, K. H., Hardy, M. Non-invasive video imaging for interrogating pharmaceutical crystallization processes. *Microscopy Microanalysis.* 2000;6(2):996-997.

12. Simon LL, Merz T, Dubuis S, Lieb A, Hungerbuhler K. In-situ monitoring of pharmaceutical and specialty chemicals crystallization processes using endoscopy-stroboscopy and multivariate image analysis. *Chem Eng Res Des.* 2012;90:1847-1855.

13. Ma CY, Wang XZ. Model identification of crystal facet growth kinetics in morphological population balance modeling of Lglutamic acid crystallization and experimental validation. *Chem Eng Sci.* 2012;70:22-30.

14. Black SN, Gray DL. Sensors and Science in Crystallisation of Pharmaceuticals. Paper presented at: 7th World Congress of Chem. Eng. 2005; Scotland.
15. Larsen PA, Rawlings JB, Ferrier NJ. Model-based object recognition to measure crystal size and shape distributions from in situ video images. *Chem Eng Sci.* 2007;62:1430 – 1441.
16. Gorpas D, Politopoulos K, Yova D. A binocular machine vision system for three-dimensional surface measurement of small objects. *Comput Med Imag Grap.* 2007;31:625-637.
17. Kempkes M, Vetter T, Mazzotti M. Measurement of 3D particle size distributions by stereoscopic imaging. *Chem Eng Sci.* 2010;65:1362-1273.
18. Bujak B, Bottlinger M. Three-dimensional measurement of particle shapes. *Part Part Syst Char.* 2008;25:293-297.
19. Boersma SM, van den Heuvel FA, Cohen AF, Scholtens REM. Photogrammetric wound measurement with a three-camera vision system. *Int Arch Photogramm Remote Sens.* 2000;33(B5/1):84-91.
20. Nedevschi S, Vancea C, Marita T, Graf T. Online extrinsic parameters calibration for stereovision systems used in far-range detection vehicle applications. *IEEE Trans Intell Transp Syst.* 2007;8(4):651-660.
21. Ballantyne GH, Moll F. The da Vinci telerobotic surgical system: the virtual operative field and telepresence surgery. *Surg Clin N Am.* 2003;83(6):1293 -1304.
22. Butner SE, Ghodoussi M. A real-time system for telesurgery. Paper presented at: International conference on distributed computing systems 2001; Mesa, AZ, USA.
23. Singh MR, Chakraborty J, Nere N, Tung H-H, Bordawekar S, Ramkrishna D. Image-analysis-based method for 3D crystal morphology measurement and polymorph identification using confocal microscopy. *Cryst Growth Des.* 2012;12:3735-3748.
24. Eggers J, Kempkes M, Cornel J, Mazzotti M, Koschinski I, Verdurand E. Monitoring size and shape during cooling crystallization of ascorbic acid. *Chem Eng Sci.* 2009;64:163-171.
25. Schorsch S, Vetter T, Mazzotti M. Measuring multidimensional particle size distributions during crystallization. *Chem Eng Sci.* 2012;77:130-142.
26. Borchert C, Temmel E, Eisenschmidt H, Lorenz H, Seidel-Morgenstern A, Sundmacher K. Image-based in situ identification of face specific crystal growth rates from crystal populations. *Cryst Growth Des.* 2014;14:952-971.
27. Karimian G, Raie AA, Faez K. A new efficient stereo line segment matching algorithm based on more effective usage of the photometric, geometric and structural information. *IEICE Trans Inf Syst.* 2006;E89-D(7):2012-2020.
28. Canny J. A computational approach to edge detection. *IEEE Trans Pattern Anal Mach Intell.* 1986;8(6):679-698.
29. Gonzalez RC, Woods RE. *Digital image processing.* 2nd ed ed. Upper Saddle River: Prentice Hall; 2002.
30. Kwon JS-I, Nayhouse M, Christofides PD, Orkoulas G. Modeling and control of shape distribution of protein crystal aggregates. *Chem Eng Sci.* 2013;104:484-497.
31. Kwon JS-I, Nayhouse M, Christofides PD, Orkoulas G. Modeling and control of crystal shape in continuous protein crystallization. *Chem Eng Sci.* 2014;107:47-57.
32. Kwon JS-I, Nayhouse M, Orkoulas G, Christofides PD. Crystal shape and size control using a plug flow crystallization configuration. *Chem Eng Sci.* 2014;119:20-39.
33. Ma CY, Wang XZ. Crystal growth rate dispersion modelling using morphological population balance. *AIChE Journal.* 2008;54(9):2321-2334.
34. Ma CY, Wang XZ, Roberts KJ. Morphological population balance for modelling crystal growth in individual face directions. *AIChE Journal.* 2008;54(1):209-222.

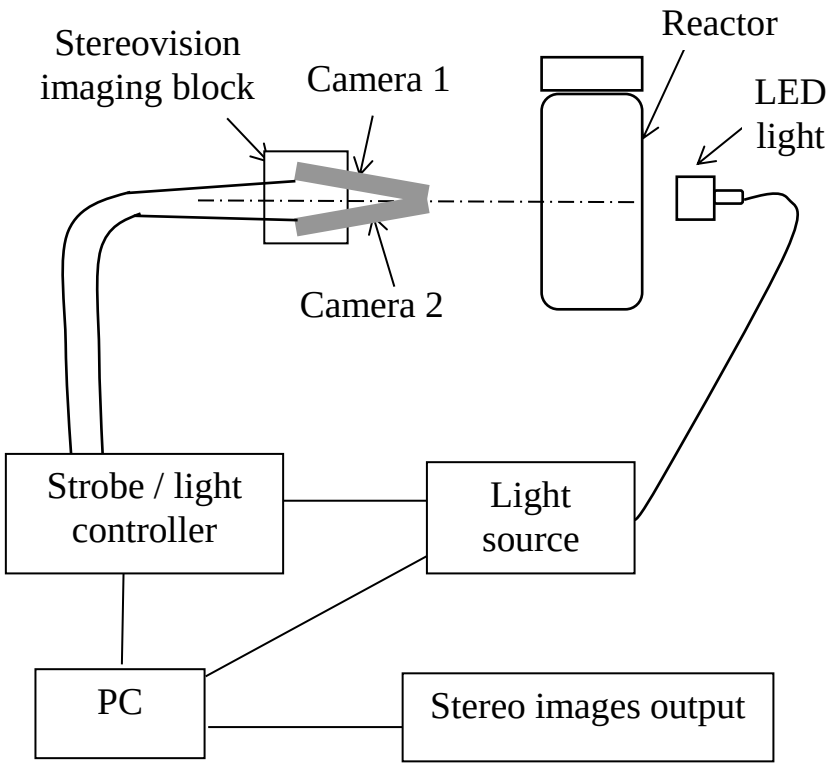

Figure 1. Schematic of the stereovision imaging system

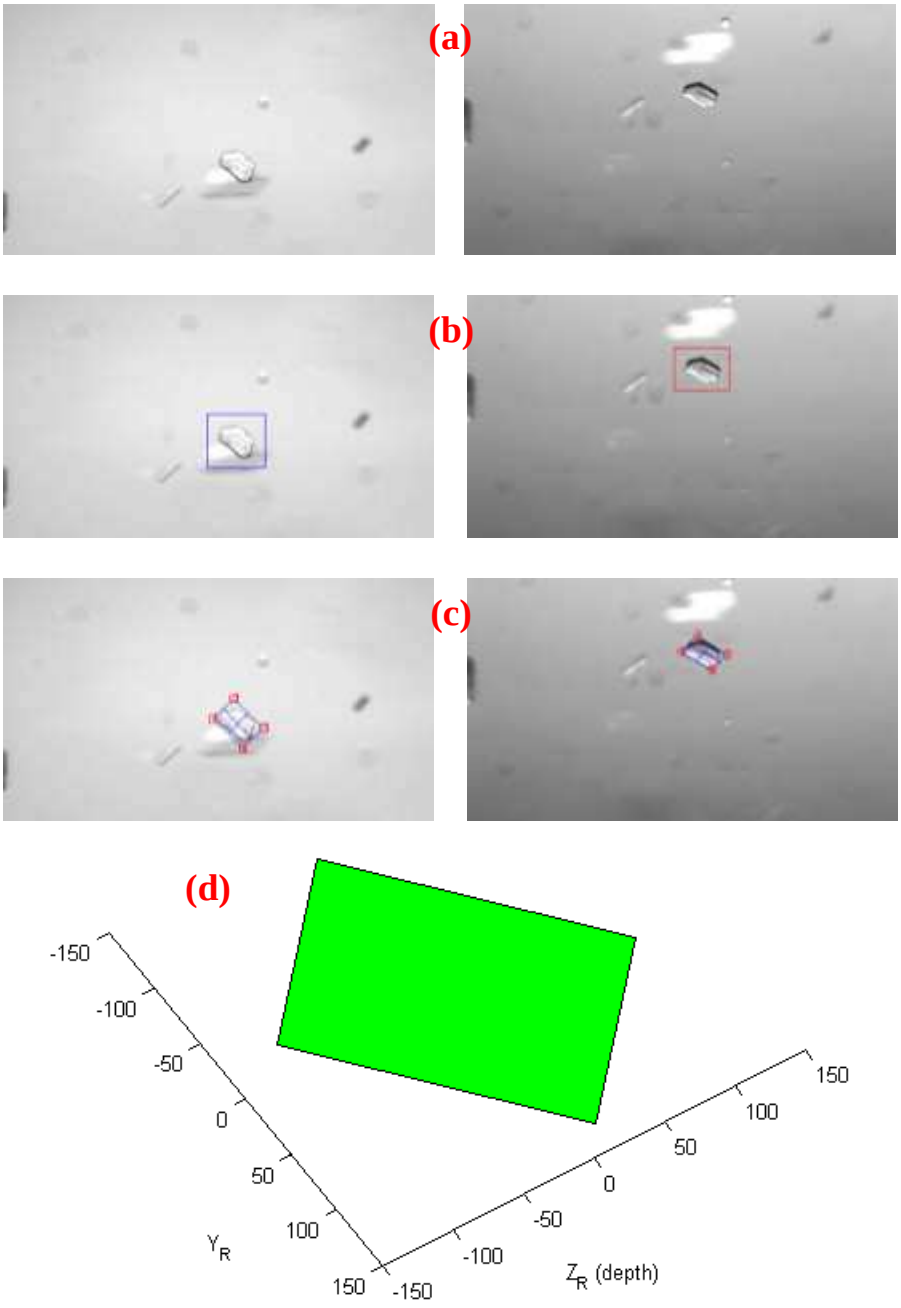

Figure 2. Shape reconstruction procedure demonstrated for a plate-like crystal (a) original image pairs, (b) identified crystal pairs, (c) feature-based edge/corner detection and correspondence, (d) reconstructed plate-like crystal in 3D space.

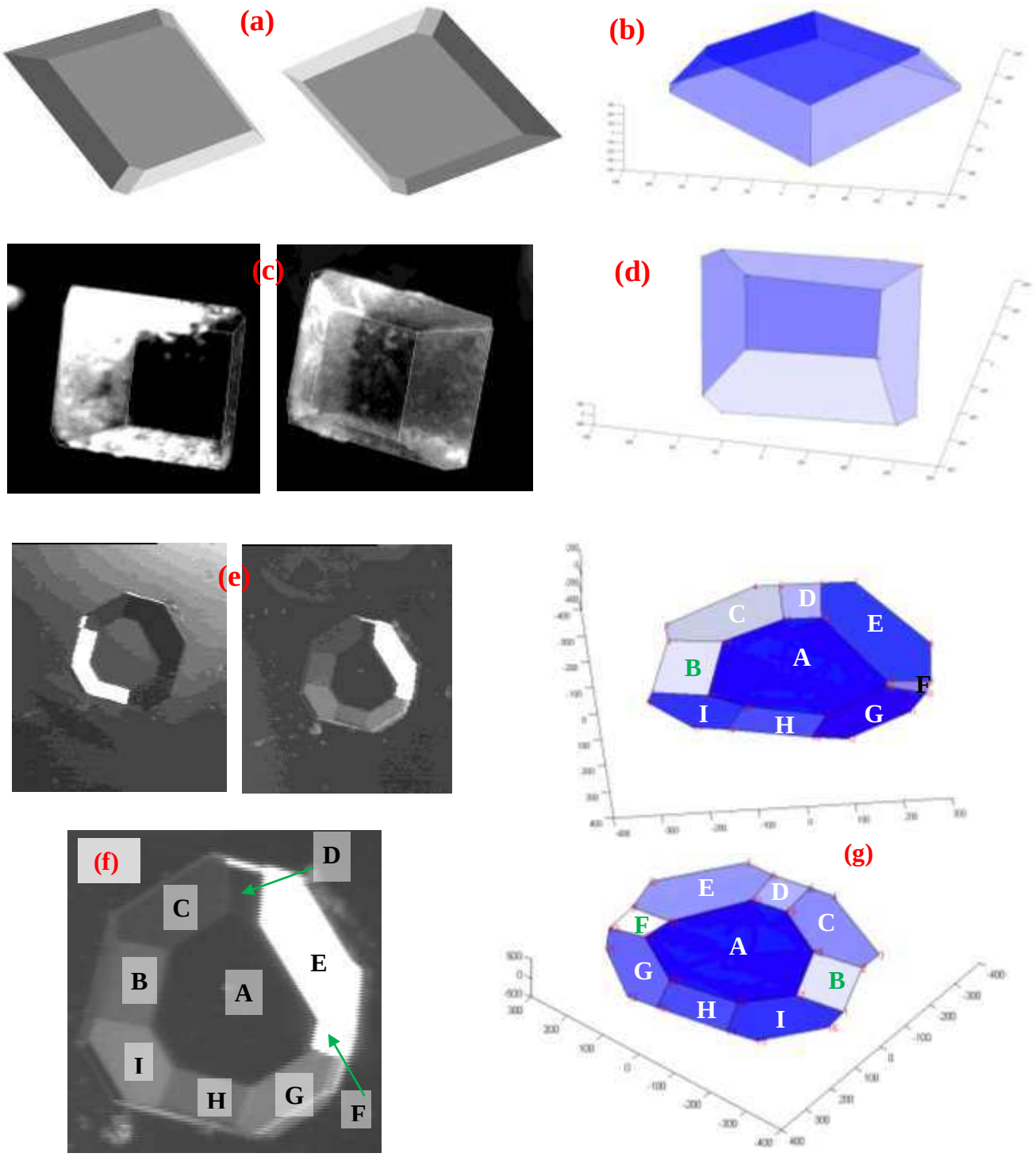

Figure 3. Examples of 3D shape reconstruction of crystals: L-glutamic acid (LGA) α crystal ((a) and (b)), Sugar ((c) and (d)), and Potash alum ((e), (f) and (g)) [(a) original 2D images of a LGA α crystal; (b) reconstructed LGA α crystal in 3D ; (c) 2D image pairs of a sugar crystal; (d) reconstructed 3D sugar crystal (e) 2D image pairs of a potash alum crystal; (f) a 2D image with nine faces; (g) reconstructed 3D crystal with two orientations (nine surfaces on the top part of the crystal: one {100} face – A; four {110} faces – B, D, F, H; and four {111} faces – C, E, G, I)]

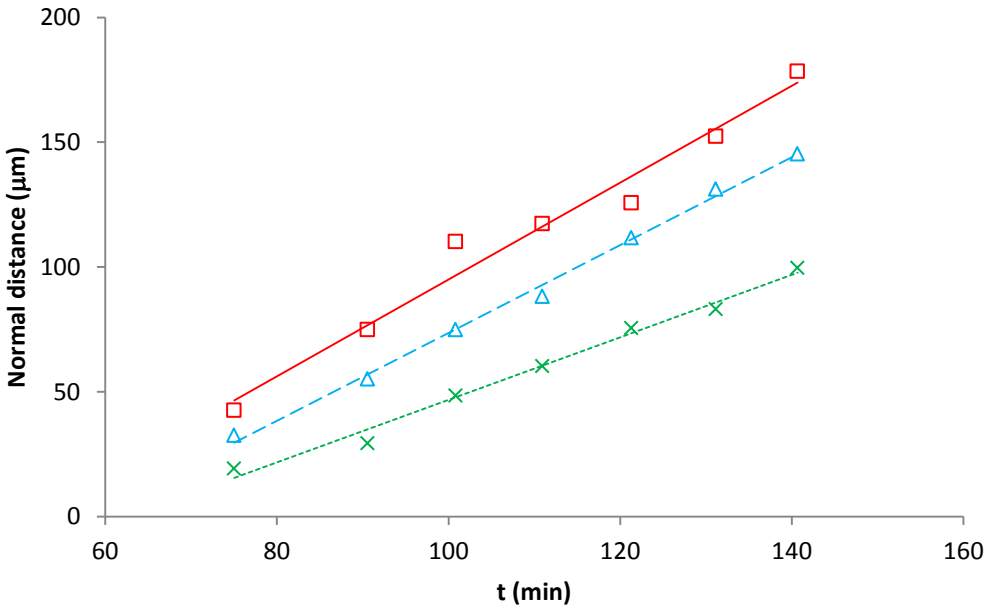

Figure 4. The evolution of the mean normal distances of individual crystal faces during the crystallisation process (symbols – reconstructed normal distances with blue triangles for face 1, red squares for face 2 and green crosses for face 3; lines – fitted normal distances with solid line for face 1 (R^2 = 0.97), dashed line for face 2 (R^2 = 0.99) and dotted line for face 3 (R^2 = 0.98))